ACS Macro Letters

Letter

pubs.acs.org/macroletters

Aspect-Ratio Effect of Nanorod Compatibilizers in Conducting Polymer Blends

Taegyun Kwon,[†,§] Kang Hee Ku,[†,§] Dong Jin Kang,[†] Won Bo Lee,[‡] and Bumjoon J. Kim*[,†]

[†]Department of Chemical and Biomolecular Engineering, Korea Advanced Institute of Science and Technology (KAIST), Daejeon, 305-701 Republic of Korea

[‡]Department of Chemical and Biomolecular Engineering, Sogang University, Seoul, 121-742 Republic of Korea

Supporting Information

ABSTRACT: Nanoparticles (NPs) at the interface between two different polymer blends or fluid mixtures can function as compatibilizers, thereby dramatically improving the interfacial properties of the blends or the fluid mixtures. Their compatibilizing ability is strongly dependent on their size, shape, and aspect ratios (ARs), which determines their adsorption energy to the interface as well as their entropic penalty when they are being strongly segregated at the interface. Herein, we investigated the effect of the ARs of nanorod surfactants on the conducting polymer blend of poly(triphenylamine) (PTPA) templated by polystyrene (PS) colloids. The lengths of the polymer-coated CuPt nanorods (CuPt NRs) were 5, 15, and 32 nm with a fixed width of 5 nm, thus producing three different AR values of 1, 3, and 6, respectively. For quantitative analysis, the morphological and electrical behaviors of the polymer blends were investigated in terms of the volume fraction and AR of the NRs. The dramatic change in the morphological and electrical properties of the blend film was observed for all three NR surfactants at the NR volume fraction of approximately 1 vol %. Therefore, NR surfactants with larger ARs had better compatibilizing power for a given number of NRs in the blends. Also, they exhibited a stronger tendency to be aligned parallel to the PS/PTPA interface. Also, we demonstrated the successful use of the NR surfactants in the fabrication of conducting polymer blend film that requires only minimal concentrations of conducting polymers. To the best of our knowledge, this is the first report of an experiment on the AR effect of NR compatibilizers in polymer blends.

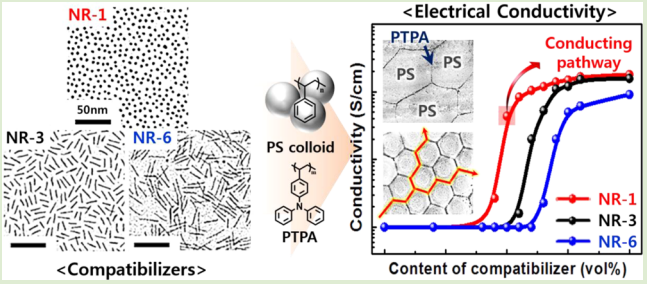

Combining the functionality of nanoparticles (NPs) with the processability of polymers holds great promise for designing novel materials with enhanced optical,[1−3] electrical,[4] magnetic,[5] and medical properties.[6] In particular, NPs with tailored surface properties can effectively modify the interface between two distinct polymers or immiscible fluids, thereby functioning as efficient surfactants in polymer blends and producing novel functional materials with enhanced properties.[7−17] One of the main advantages of NP surfactants over conventional compatibilizers (i.e., block and graft copolymers) is their quasi-irreversible adsorption to the polymer−polymer interface, which produces extremely stable morphologies.[18−20] The final morphology of polymer blends with NP surfactants is determined by complex interplay between the entropic and enthalpic interactions within the system. This interplay can be tuned by controlling the size, shape, and surface chemistry of the NPs that determine the adsorption energy (E_a) of the NPs to the interface.[21,22] In this regard, we recently studied the size effect of the NPs on the interfacial properties and morphological behavior of polymer blends.[19] The surface properties of NPs can be tailored by end-attaching organic/polymeric ligands to the surface of the NPs to produce their strong segregation to the interface between the polymer blends.[13,23−26]

Recently, NR-based polymer nanocomposites have attracted great attention primarily because of their unique and inherent physical properties that originate from the one-dimensional shape of the NRs.[27−32] For example, noble metal NRs, such as gold or silver, are optically active due to the excitation of surface plasmons in the NRs, and such optical behavior can be enhanced by controlling the size and shape of the NRs.[33−37] In addition, semiconducting NRs, which contribute to the efficient formation of electrical pathways, can improve the efficiency of polymer solar cells by increasing carrier mobility within the device.[38,39] The shape anisotropy provides many opportunities for enhancing carrier mobility that are not possible for isotropic shapes.[40−42] For example, when electrically conductive carbon nanotubes (CNTs) are incorporated in a homopolymer matrix or used as a separate network of conducting nanorods with the help of the polymer colloidal template, they can produce a significant improvement in the electrical properties of polymer

Received: January 15, 2014
Accepted: April 2, 2014
Published: April 8, 2014

   dx.doi.org/10.1021/mz500024n | *ACS Macro Lett.* 2014, 3, 398−404

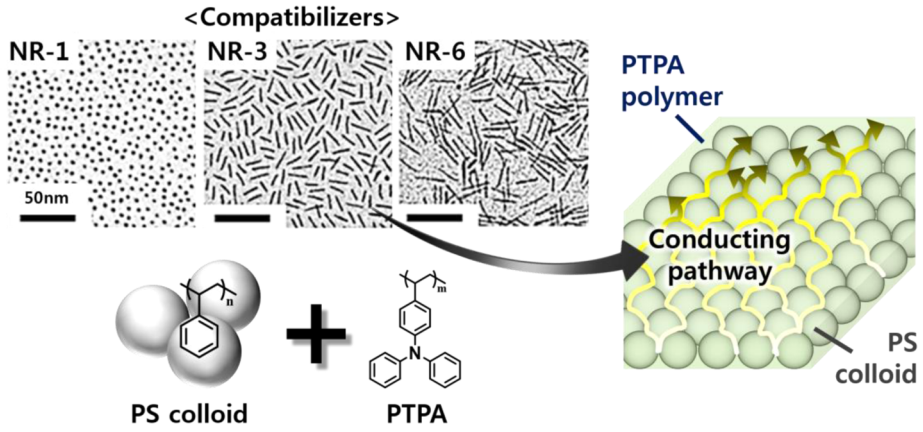

Figure 1. Schematic representation of the experimental system: CuPt NRs with three different AR values and their application in the PS colloid/PTPA blend; (upper) TEM images of P(S-*b*-SN_3)-coated CuPt NRs with various ARs. The polymer-coated CuPt NRs had average ARs of 1.0 (NR-1), 3.2 (NR-3), and 5.9 (NR-6). The scale bars are 50 nm.

Table 1. Characteristics of the Polymer-Coated CuPt NRs Used in This Study

list	aspect ratio	type	length (nm)	width (core + shell) (nm)	polymer shell thickness[a] (nm)	Σ^a (chain/nm^2)
NR-1	1.0	sphere	5.0	5.0	1.2	0.38
NR-3	3.2	cylinder	16.7	5.2	1.4	0.33
NR-6	5.9	cylinder	32.2	5.5	1.5	0.34

[a]Analysis obtained from TGA data.

composites at low percolation thresholds.[30,43−45] Moreover, if the surface properties of the NRs can be well tailored and their positioning can be precisely controlled within the polymeric domain, they can bring a critical influence on the interfacial and electrical properties of the composites.[46,47] Recently, the influence of NRs in the morphological behavior of the polymer blends has been studied by numerical simulation.[48−50] In particular, Yang et al. used dissipative particle dynamics simulations to study the compatibilizing effect of NRs in polymer blends.[49] It was found that NR surfactants effectively broadened the interfacial width and reduced the interfacial tension, the effect of which was strongly dependent on the aspect ratio (AR) of the NRs. However, experiments to determine the AR effects of the NRs on the interfacial and morphological properties of immiscible polymer blends have not been conducted to date.

In this work, we studied the effect of the three different ARs of the polymer-coated CuPt NRs on the morphological and electrical properties of the conducting polymer blends. Also, we demonstrated the use of the CuPt NRs as surfactants in the fabrication of conducting polymer blend films that have the desired electrical properties and superior stabilities. A polymer blend consisting of polystyrene (PS) colloids and poly(triphenylamine) (PTPA) was designed as a model system for investigating the AR effect of the NRs on the immiscible polymer blends. This choice was made for two important reasons, that is, (1) the morphological changes of the blend caused by the NR surfactants can be easily monitored by measuring the degree of infiltration of the PTPA polymer into the PS template and (2) a macroscopic view of the morphological change of the polymer blend by the NR surfactants can be precisely provided by measuring the electrical conductivity of the blends in a large area of the film. Figure 1 illustrates the experimental system of the PS colloid/PTPA blend containing AR-controlled CuPt NR surfactants.

In order to generate a model system to elucidate the AR effect of the NRs on the blends, we first synthesized a series of oleic acid/oleylamine coated CuPt NRs with ARs of 1.0, 5.6, and 11.3 by the thermal decomposition method with the standard air-free technique.[51,52] Figure S1 of the Supporting Information shows that the CuPt NRs were highly monodisperse and the core of the CuPt NRs had the same width (2.5 nm). Then, the CuPt NRs were coated with thiol-terminated polystyrene-*b*-poly(4-azidostyrene) P(S-*b*-SN_3) block copolymer via a ligand-exchange process. The thiol-terminated P(S-*b*-SN_3) polymer was synthesized by reversible addition−fragmentation chain transfer (RAFT) polymerization to produce a total molecular weight (M_n) of 4500 g/mol and a polydispersity index (PDI) of 1.10 (Figure S2).[53,54] Because the grafting density of the P(S-*b*-SN_3) chains on the CuPt NR cores (Σ) was a critical parameter to determine their surface properties and interaction with the polymer matrix, the Σ values for all three P(S-*b*-SN_3)-coated CuPt NRs were kept approximately at 0.35 chain/nm^2.[24,55] Figures 1 shows the TEM images of the polymer coated CuPt NRs with three different ARs of 1.0 (NR-1), 3.2 (NR-3), and 5.9 (NR-6). The overall (polymer shell + CuPt NR core) ARs of the three different CuPt NRs were determined to be 1.0, 3.2, and 5.9, respectively, by considering the thickness of the grafted P(S-*b*-SN_3) shell. Thus, the AR ratios (1.0:3.2:5.9) of the polymer coated CuPt NRs are different from those (1.0:5.6:11.3) of the bare CuPt NRs. Both the thickness and the Σ value of the polymer shell were estimated based on the core size of the CuPt NRs, and the relative weights of the CuPt NR cores and the polymer ligands in the CuPt NRs. The synthesized CuPt NRs were washed several times using the density gradient method[56] in order to remove any ungrafted polymeric ligands from the polymer-coated CuPt NRs and to determine the exact amount of grafted P(S-*b*-SN_3) ligands. (Figure S3). It was assumed that the entire surface of the CuPt core was coated uniformly by the polymer chains. The characteristics of three

dx.doi.org/10.1021/mz500024n | *ACS Macro Lett.* 2014, 3, 398−404

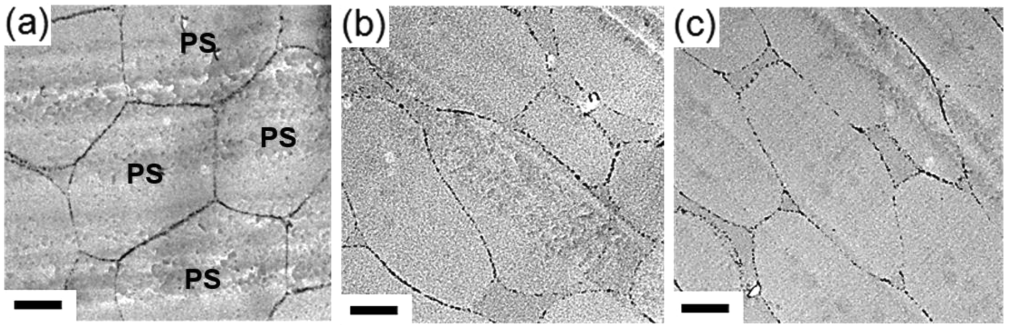

Figure 2. Cross-sectional TEM images of the PS colloid/PTPA blend film (90:10 v/v) containing ϕ_{NR} = 1.0 vol % of CuPt NRs with various ARs: (a) NR-1, (b) NR-3, and (c) NR-6. The scale bars are 500 nm.

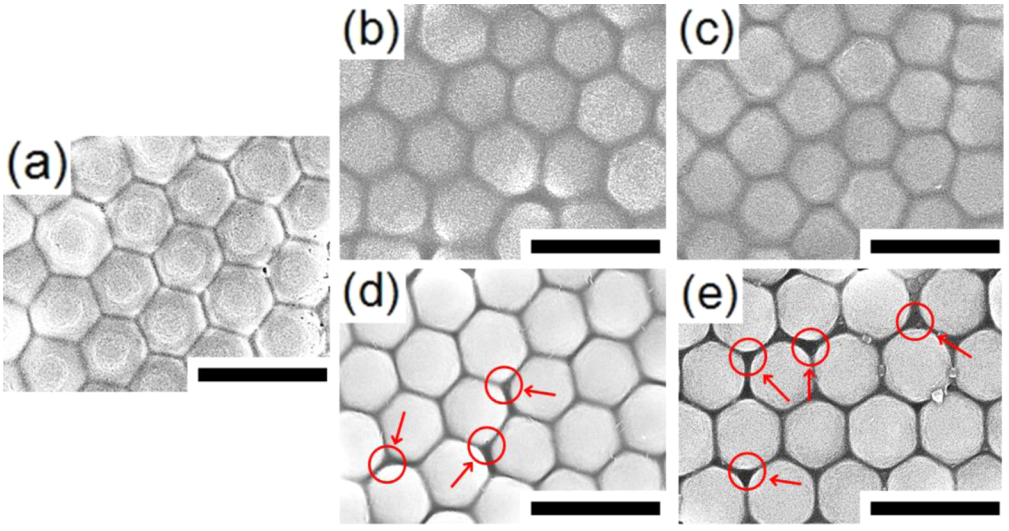

Figure 3. SEM images of PS colloid/PTPA blend films with (a) ϕ_{NR} = 0.9 vol % of NR-1, (b) ϕ_{NR} = 1.1 vol % of NR-3, (c) ϕ_{NR} = 1.3 vol % of NR-6, (d) ϕ_{NR} = 0.9 vol % of NR-3, and (e) ϕ_{NR} = 0.9 vol % of NR-6. Scale bars are 5 μm. The red arrows indicate some of the voids in the film.

different polymer-coated CuPt NRs are summarized in Table 1. It is noted that the P(S-*b*-SN_3)-coated CuPt NRs satisfied important requirements for their use as compatibilizers in the PS/PTPA system. Due to their cross-linkable PSN_3 outershell, the P(S-*b*-SN_3)-coated CuPt NRs should possess excellent thermal stability required for thermal processing of the polymer blend. In addition, the polymer-coated CuPt NRs have a balanced enthalpic interaction with both the PS and PTPA domains, so the CuPt NRs are strongly localized at their interface and are highly active as compatibilizers (Figure S4).[19,54]

To explore the potential of polymer-coated CuPt NRs as compatibilizers in the polymer blends, a series of PS colloid/PTPA blend samples with a fixed volume ratio of 90:10 was prepared with the addition of different types of NR-1, NR-3, and NR-6. Cross-linked PS colloids with diameters of 2.5 μm were synthesized and used as a template to produce the continuous PTPA phase.[10] Figure 2 presents cross-sectional TEM images of the PS colloid/PTPA blends (90:10 v/v) containing (a) NR-1, (b) NR-3, and (c) NR-6. The volume fraction of the NRs in the blend (ϕ_{NR}) was fixed at 1.0 % for the three samples. All three samples of the CuPt NRs exhibited excellent dispersibility with strong segregation at the interface between the two distinct phases of the PS colloids and PTPA. Interestingly, the lightly cross-linked PS colloids were deformed and reorganized to polyhedron shapes that were wetted by low volume fraction of the PTPA phase upon thermal annealing. Thus, the CuPt NRs functioned effectively as compatibilizers by reducing the interfacial tension and tailoring the morphological properties of the blends. This feature was consistent with the findings of a previous study in which other types of surfactants were used.[10,57]

Various samples of the PS colloid/PTPA blend containing NR-1, NR-3, and NR-6 with different ϕ_{NR} values were prepared, and their morphologies were compared by scanning electron microscopy (SEM). All samples were prepared at identical conditions, including the annealing condition of 170 °C for 8 h. Figure 3 shows representative SEM images of the PS colloid/PTPA blend (90:10 v/v) containing ϕ_{NR} values of (a) 0.9 vol % of NR-1, (b) 1.1 vol % of NR-3, (c) 1.3 vol % of NR-6, (d) 0.9 vol % of NR-3, and (e) 0.9 vol % of NR-6. The addition of NR-1 with ϕ_{NR} = 0.9 vol % (Figure 3a) produced nicely organized PS colloid polyhedrons, thereby inducing the complete infiltration of the PTPA phase surrounding the PS colloids, which is in contrast to the case without the NR compatibilizers shown in Figure S5 of the Supporting Information. The observed morphological transition was associated with the significantly reduced interfacial tension that was driven by the strongly segregated CuPt NR compatibilizers. The formation of continuous PTPA network in the PS colloids/PTPA blend was also obtained by the addition of NR-3 and NR-6 (Figure 3b and c). Therefore, all of the CuPt NRs were interfacially active to induce dramatic morphological transitions. Interestingly, the ϕ_{NR} values

dx.doi.org/10.1021/mz500024n | *ACS Macro Lett.* 2014, 3, 398−404

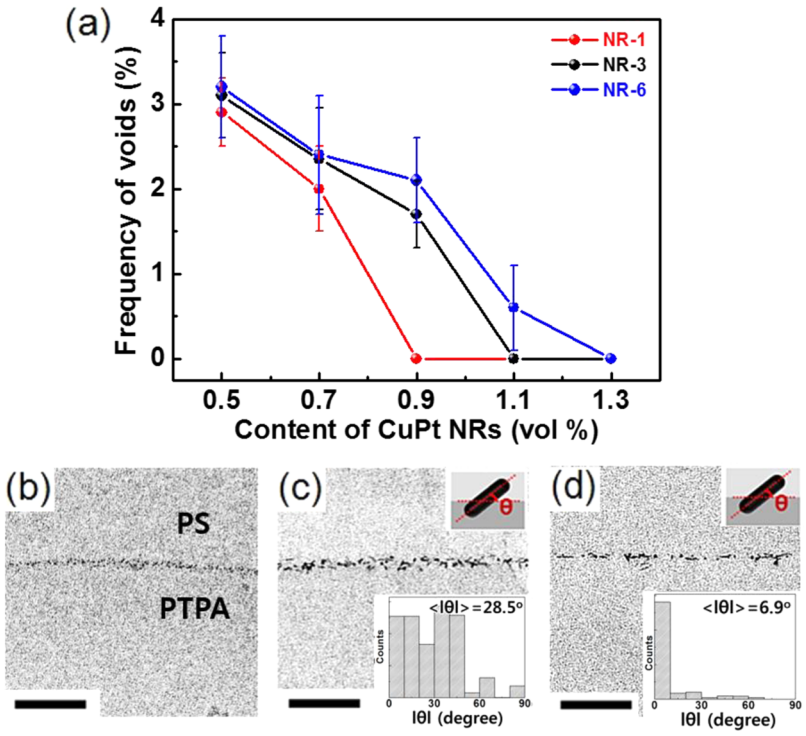

Figure 4. (a) Frequency of voids in the PS colloid/PTPA blends as a function of the ϕ_{NR} values of CuPt NRs. Parts b–d show cross-sectional TEM images of PS/PTPA bilayer film with different CuPt NRs. All of CuPt NRs were strongly segregated and preferentially oriented parallel to the PS/PTPA interface. The ϕ_p values of (b) NR-1, (c) NR-3, and (d) NR-6 were kept the same (0.9 vol %). The scale bars are 100 nm. The statistics of orientational distribution of the CuPt NRs at the interface are shown in the insets.

required for such morphological transition were different for NR-1, NR-3, and NR-6. Figure 3a, d, and e compares the PS colloid/PTPA blend film at the same ϕ_{NR} of 0.9 vol %, but with different NRs. The surfaces of the PS colloids were partially wetted by the PTPA phase for the cases of NR-3 and NR-6 at the ϕ_{NR} value of 0.9 vol %. The voids between the PS colloids disappeared completely with the higher ϕ_{NR} values of 1.1 vol % (NR-3) and 1.3 vol % (NR-6).

To obtain a quantitative comparison of the compatibilizing effect in relation to the ARs of the CuPt NRs, the frequency of the voids in the PS colloids/PTPA blend was measured statistically from the SEM images of the blend films and plotted as a function of ϕ_{NR} for the three different NRs (Figure 4). The frequency of voids was obtained by image analysis from more than 300 particle units for each sample. For all of the NRs, the frequency of the voids decreased dramatically as the ϕ_{NR} value increased. However, the critical NR volume fractions ($\phi_{NR,C}$), at which all of the voids were removed to provide a continuous PTPA network, were found to be slightly different for three NRs. The $\phi_{NR,C}$ values for NR-1, NR-3, and NR-6 were observed to be 0.9, 1.1, and 1.3 vol %, respectively. This feature can be partly understood by considering the difference in the interfacial area occupied by the different NRs. For this purpose, we measured the orientational distribution of the anisotropic NRs at the PS/PTPA interface. It should be noted that, to remove any curvature effect imposed by the PS colloids on the orientational distribution of the NRs at the PS/PTPA interface, a bilayer sample of PS and PTPA homopolymers was prepared as described in the Supporting Information. Three different NR-1, NR-3, and NR-6 were added with a fixed ϕ_{NR} value of 0.9 vol % and prepared at the same annealing conditions (170 °C for 8 h). Figure 4b–d show the cross-sectional TEM images of the NR-1, NR-3, and NR-6 within the PS/PTPA bilayer film.

The statistics of the orientational distribution of the CuPt NRs were obtained by analyzing the TEM images and counting more than 1000 particles for each sample. While spherical particles had no orientational distributions, anisotropic NR-3 and NR-6 had them with average values of absolute angles ($\langle|\theta|\rangle$ = 28.5°, and 6.9°, respectively), with respect to the interfacial plane. The orientational distributions are one of reasons that, at the same ϕ_{NR} value, the interfacial area of the PS/PTPA occupied by NR-3 and NR-6 should be lower than that occupied by the spherical NR-1. This feature explains why the $\phi_{NR,C}$ value for NR-1 (0.9 vol %) was lower than those of NR-3 and NR-6.

The decreasing trend of rotational angle for the NRs with larger AR values can be understood by comparing the two different free energy gains in which the NRs were oriented parallel and perpendicular to the interface. According to Pieranski's argument, for NR surfactants parallel or perpendicular to the PS/PTPA interface, the adsorption energy difference at the interface (i.e., ΔE_{par} and ΔE_{per}) from the state that NR surfactants are immersed in PS homopolymers can be expressed as shown below:[22,58]

$$\Delta E_{par} = -2RL \sin\theta\gamma_{PS/PTPA} + 2RL\theta(\gamma_{NR/PTPA} - \gamma_{NR/PS})$$
$$\text{where} \quad \cos\theta = \frac{\gamma_{NR/PTPA} - \gamma_{NR/PS}}{\gamma_{PS/PTPA}} \quad (L \gg R) \tag{1}$$

$$\Delta E_{per} = (\gamma_{NR/PTPA} - \gamma_{PS/PTPA} - \gamma_{NR/PS})\pi R^2 + (\gamma_{NR/PTPA} - \gamma_{NR/PS})2\pi Rh \tag{2}$$

where R and L are the radius and length of the NR surfactant, respectively, and γ denotes the interfacial energy between the

dx.doi.org/10.1021/mz500024n | ACS Macro Lett. 2014, 3, 398–404

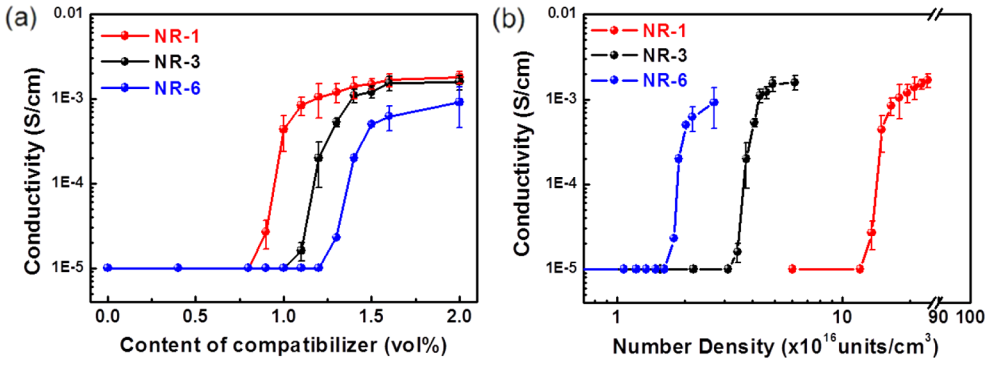

Figure 5. Conductivities of the PS colloid/PTPA films as a function of (a) the ϕ_{NR} values of the CuPt NRs and (b) the number density of the CuPt NRs.

two phases; cos θ is the ratio of the difference in γ between the NRs and the two homopolymers to that between the PS and PTPA phases; and h is the immersion depth of the NRs into the PTPA phase when assembled normal to the interface. To evaluate the values of ΔE_{par} and ΔE_{per} for different NRs, the interfacial tensions (γ) of PS, PTPA, and the CuPt NRs were calculated based on the Wu model (Supporting Information, Tables S2−4).[59,60] By substituting each interfacial tension value ($\gamma_{PS/PTPA}$ = 0.40 mJ/m^2, $\gamma_{NR/PS}$ = 0.06 mJ/m^2, and $\gamma_{NR/PTPA}$ = 0.14 mJ/m^2) into the eqs 1 and 2, the values of ΔE_{par} and ΔE_{per} for each different NR-3 and NR-6 units were calculated. The values of ΔE_{par} and ΔE_{per} for NR-3 were -2.45×10^{-17} and 4.12×10^{-18} mJ/unit, respectively, while the longer NR-6 had ΔE_{par} and ΔE_{per} values of -5.00×10^{-17} and 1.47×10^{-17} mJ/unit, respectively. For both NR-3 and NR-6, the positioning of the NRs that were oriented perpendicular to the PS/PTPA interface was accompanied by significant energy penalties. In contrast, the free energy of the system can be significantly reduced by the addition of the NR surfactants parallel to the interfacial plane. Therefore, the NR surfactants were oriented preferentially to be parallel to the interfacial plane rather than perpendicular to it to minimize the free energy of the system, which is mainly due to the reduction of the PS/PTPA interfacial area caused by the NR surfactants. Also, NR-6, with the larger AR value, had a stronger trend toward being parallel-oriented to decrease the orientational distribution.[49] However, despite better alignment of NR-6 parallel to the interface of the PS/PTPA bilayer film, the $\phi_{NR,C}$ value for NR-6 was slightly higher than that for NR-3 in the PS colloid/PTPA blend. This feature probably can be attributed to the fact that the highly anisotropic NRs often tend to aggregate side-by-side due to the rod−rod interactions including the depletion forces and the van der Waals interaction, which could generate another contribution to the discrepancy in the actual interfacial coverage of the NRs.[27,32,34]

To gain a deeper insight of the compatibilizing effect of the AR-controlled NRs, the electrical conductivities of the PS colloid/PTPA blends with different ARs were measured and compared. Because each sample used for conductivity measurements covered a large area (1.8 cm × 0.5 cm) between the electrodes, a macroscopic view of the compatibilizing effect of the NRs on the PS colloid/PTPA film can be identified by the conductivity measurement. Figure 5a shows the conductivities of the films as a function of ϕ_{NR} for different NRs. A pristine PS colloid/PTPA system (90:10 v/v) without any surfactants had incomplete infiltration of the PTPA phases into the spaces among the PS colloids; thus, the electrical conductivity could not be measured because the surface resistivity was too high. In contrast, a dramatic increase in conductivity occurred for all of the compatibilized blends above certain values of ϕ_{NR}. At this point, called the "percolation threshold", a remarkable change appeared in the morphology of the blend due to the formation of an infinite network of PTPA through the insulating matrix, and holes begin to flow through the conducting PTPA pathway. Of particular interest was that the values of the percolation threshold for NR-1, NR-3, and NR-6 were determined to be 0.9, 1.1, and 1.3 vol %, respectively. These values are in excellent agreement with the $\phi_{NR,C}$ values from the morphological study shown in Figure 4a.

To compare the compatibilizing power of each AR-controlled NR unit quantitatively, we plotted the conductivity of the PS colloid/PTPA blend as a function of the number density (N_{NR}) of the NR compatibilizer (Figure 5b). For the calculation, it was assumed that an individual NR was a cylindrical body with the ends capped by hemispheres. Also, the radius and length of the cylinder, as well as the radius of the hemisphere, were the values shown in Table 1. The NR-6 had the lowest percolation threshold value of $N_{NR} = 1.8 \times 10^{16}$/cm^3, while the NR-3 and NR-1 had higher values of $N_{NR} = 3.5 \times 10^{16}$/cm^3 and $N_{NR} = 1.4 \times 10^{17}$/cm^3, respectively, at the percolation threshold. The results indicated that an individual NR compatibilizer with a larger AR exhibited much stronger compatibilizing power. Also, we calculated and compared the interfacial coverage (A_C) at the PS colloid/PTPA interface occupied by the CuPt NRs. The A_C values were estimated from the total cross-sectional area of the CuPt NRs at the PS/PTPA interface considering the length of the NRs as well as their orientational distribution at the interface (Figure S6). Interestingly, the A_C ratios for NR-1, NR-3, and NR-6 with same number of NR units were calculated as 1:3.4 (±0.8):8.4 (±0.9). These ratios can explain the difference of the N_{NR} values for three NRs at the percolation threshold as shown in Figure 5b. All of the CuPt NRs were highly efficient compatibilizers for the fabrication of continuous conducting polymer films that require minimal amount of PTPA polymer and thus have enhanced stabilities.[61]

In conclusion, comparisons of three different CuPt NR-1, NR-3, and NR-6 were used to elucidate the effects of the ARs of the NR compatibilizers on the morphological and electrical properties of the PS colloids/PTPA blend. NR-1, NR-3, and NR-6 had the same width (5 nm) and surface properties with similar Σ values, but they had different lengths, which produced a model system in which to observe the AR effect of the NR compatibilizers. The $\phi_{NR,C}$ value for the morphological

dx.doi.org/10.1021/mz500024n | ACS Macro Lett. 2014, 3, 398−404

transition in the formation of the continuous PTPA phase within the PS colloid template was determined to be 0.9, 1.1, and 1.3 vol % for NR-1, NR-3, and NR-6, respectively. The values were in excellent agreement with the numbers for the dramatic increase in the electrical properties. Thus, the NR surfactant with the larger AR exhibited stronger compatibilizing power compared to one with a smaller AR for a given number of NRs. We demonstrated the use of the NR surfactants in the fabrication of conducting polymer blend films that required only minimal concentrations of conducting polymers, thus exhibiting excellent electrical properties and superior stabilities.

■ ASSOCIATED CONTENT

Supporting Information

Materials and methods, detailed experimental procedures, and additional data. This material is available free of charge via the Internet at http://pubs.acs.org.

■ AUTHOR INFORMATION

Corresponding Author

*E-mail: bumjoonkim@kaist.ac.kr.

Author Contributions

§T.K. and K.H.K. contributed equally.

Notes

The authors declare no competing financial interest.

■ ACKNOWLEDGMENTS

This research was supported by the Korean Research Foundation Grant by the Korean Government (2013R1A2A1A03069803). This work was also supported by Samsung Research Funding Center of Samsung Electronics under Project Number SRFC-MA1301-07.

■ REFERENCES

(1) Bockstaller, M. R.; Thomas, E. L. *Phys. Rev. Lett.* **2004**, *93*, 166106.
(2) Wilson, O.; Wilson, G. J.; Mulvaney, P. *Adv. Mater.* **2002**, *14*, 1000.
(3) Shenhar, R.; Norsten, T. B.; Rotello, V. M. *Adv. Mater.* **2005**, *17*, 657.
(4) Balazs, A. C.; Emrick, T.; Russell, T. P. *Science* **2006**, *314*, 1107.
(5) Shin, S.; Jang, J. *Chem. Commun.* **2007**, 4230.
(6) Sambhy, V.; MacBride, M. M.; Peterson, B. R.; Sen, A. *J. Am. Chem. Soc.* **2006**, *128*, 9798.
(7) Ikem, V. O.; Menner, A.; Bismarck, A. *Angew. Chem.* **2008**, *120*, 8401.
(8) Chen, T.; Colver, P. J.; Bon, S. A. F. *Adv. Mater.* **2007**, *19*, 2286.
(9) Gubbels, F.; Jerome, R.; Teyssie, P.; Vanlathem, E.; Deltour, R.; Calderone, A.; Parente, V.; Bredas, J. L. *Macromolecules* **1994**, *27*, 1972.
(10) Kang, D. J.; Kwon, T.; Kim, M. P.; Cho, C. H.; Jung, H.; Bang, J.; Kim, B. J. *ACS Nano* **2011**, *5*, 9017.
(11) Miesch, C.; Kosif, I.; Lee, E.; Kim, J. K.; Russell, T. P.; Hayward, R. C.; Emrick, T. *Angew. Chem., Int. Ed.* **2012**, *51*, 145.
(12) Lee, D.; Weitz, D. A. *Adv. Mater.* **2008**, *20*, 3498.
(13) Chung, H.-J.; Ohno, K.; Fukuda, T.; Composto, R. J. *Nano Lett.* **2005**, *5*, 1878.
(14) Kim, B. J.; Fredrickson, G. H.; Hawker, C. J.; Kramer, E. J. *Langmuir* **2007**, *23*, 7804.
(15) Jang, S. G.; Kim, B. J.; Hawker, C. J.; Kramer, E. J. *Macromolecules* **2011**, *44*, 9366.
(16) Kim, J.; Cote, L. J.; Kim, F.; Yuan, W.; Shull, K. R.; Huang, J. *J. Am. Chem. Soc.* **2010**, *132*, 8180.
(17) Elias, L.; Fenouillot, F.; Majeste, J. C.; Cassagnau, P. *Polymer* **2007**, *48*, 6029.
(18) Binks, B. P. *Curr. Opin. Colloid Interface Sci.* **2002**, *7*, 21.
(19) Kwon, T.; Kim, T.; Ali, F. B.; Kang, D. J.; Yoo, M.; Bang, J.; Lee, W.; Kim, B. J. *Macromolecules* **2011**, *44*, 9852.
(20) Sacanna, S.; Kegel, W. K.; Philipse, A. P. *Phys. Rev. Lett.* **2007**, *98*, 158301.
(21) Boker, A.; He, J.; Emrick, T.; Russell, T. P. *Soft Matter* **2007**, *3*, 1231.
(22) Pieranski, P. *Phys. Rev. Lett.* **1980**, *45*, 569.
(23) Shan, J.; Nuopponen, M.; Jiang, H.; Viitala, T.; Kauppinen, E.; Kontturi, K.; Tenhu, H. *Macromolecules* **2005**, *38*, 2918.
(24) Kim, B. J.; Bang, J.; Hawker, C. J.; Chiu, J. J.; Pine, D. J.; Jang, S. G.; Yang, S. M.; Kramer, E. J. *Langmuir* **2007**, *23*, 12693.
(25) Walther, A.; Matussek, K.; Muller, A. H. E. *ACS Nano* **2008**, *2*, 1167.
(26) Chung, H.-J.; Kim, J.; Ohno, K.; Composto, R. J. *ACS Macro Lett.* **2012**, *1*, 252.
(27) Li, W.; Zhang, P.; Dai, M.; He, J.; Babu, T.; Xu, Y.-L.; Deng, R.; Liang, R.; Lu, M.-H.; Nie, Z.; Zhu, J. *Macromolecules* **2013**, *46*, 2241.
(28) Vigderman, L.; Khanal, B. P.; Zubarev, E. R. *Adv. Mater.* **2012**, *24*, 4811.
(29) Chen, H.; Shao, L.; Li, Q.; Wang, J. *Chem. Soc. Rev.* **2013**, *42*, 2679.
(30) Moniruzzaman, M.; Winey, K. I. *Macromolecules* **2006**, *39*, 5194.
(31) Hore, M. J. A.; Composto, R. J. *Macromolecules* **2014**, *47*, 875.
(32) Li, L.; Miesch, C.; Sudeep, P. K.; Balazs, A. C.; Emrick, T.; Russell, T. P.; Hayward, R. C. *Nano Lett.* **2011**, *11*, 1997.
(33) Jiang, G.; Hore, M. J. A.; Gam, S.; Composto, R. J. *ACS Nano* **2012**, *6*, 1578.
(34) Hore, M. J. A.; Composto, R. J. *ACS Nano* **2010**, *4*, 6941.
(35) Funston, A. M.; Novo, C.; Davis, T. J.; Mulvaney, P. *Nano Lett.* **2009**, *9*, 1651.
(36) Liz-Marzan, L. M. *Langmuir* **2006**, *22*, 32.
(37) Mayer, K. M.; Hafner, J. H. *Chem. Rev.* **2011**, *111*, 3828.
(38) Huynh, W. U.; Dittmer, J. J.; Alivisatos, A. P. *Science* **2002**, *295*, 2425.
(39) Lin, Y.-Y.; Chu, T.-H.; Li, S.-S.; Chuang, C.-H.; Chang, C.-H.; Su, W.-F.; Chang, C.-P.; Chu, M.-W.; Chen, C.-W. *J. Am. Chem. Soc.* **2009**, *131*, 3644.
(40) Gonzalez-Valls, I.; Lira-Cantu, M. *Energy Environ. Sci.* **2009**, *2*, 19.
(41) Kang, Y. M.; Park, N. G.; Kim, D. *Appl. Phys. Lett.* **2005**, *86*, 113101.
(42) Mutiso, R. M.; Sherrott, M. C.; Rathmell, A. R.; Wiley, B. J.; Winey, K. I. *ACS Nano* **2013**, *7*, 7654.
(43) Kim, M. H.; Choi, J. Y.; Choi, H. K.; Yoon, S. M.; Park, O. O.; Yi, D. K.; Choi, S. J.; Shin, H. J. *Adv. Mater.* **2008**, *20*, 457.
(44) Vaia, R. A.; Maguire, J. F. *Chem. Mater.* **2007**, *19*, 2736.
(45) Jurewicz, I.; King, A. A. K.; Worajittiphon, P.; Asanithi, P.; Brunner, E. W.; Sear, R. P.; Hosea, T. J. C.; Keddie, J. L.; Dalton, A. B. *Macromol. Rap. Commun.* **2010**, *31*, 609.
(46) Yan, L.-T.; Maresov, E.; Buxton, G. A.; Balazs, A. C. *Soft Matter* **2011**, *7*, 595.
(47) Deshmukh, R. D.; Liu, Y.; Composto, R. J. *Nano Lett.* **2007**, *7*, 3662.
(48) Hore, M. J. A.; Laradji, M. *J. Chem. Phys.* **2008**, *128*, 054901.
(49) Yang, Z.; Long, X. P.; Zeng, Q. X. *Polymer* **2011**, *52*, 6110.
(50) Buxton, G. A.; Balazs, A. C. *Mol. Simul.* **2004**, *30*, 249.
(51) Liu, Q.; Yan, Z.; Henderson, N. L.; Bauer, J. C.; Goodman, D. W.; Batteas, J. D.; Schaak, R. E. *J. Am. Chem. Soc.* **2009**, *131*, 5720.
(52) Kwon, T.; Min, M.; Lee, H.; Kim, B. J. *J. Mater. Chem.* **2011**, *21*, 11956.
(53) Lim, J.; Yang, H.; Paek, K.; Cho, C.-H.; Kim, S.; Bang, J.; Kim, B. J. *J. Polym. Sci., Part A: Polym. Chem.* **2011**, *49*, 3464.
(54) Yoo, M.; Kim, S.; Lim, J.; Kramer, E. J.; Hawker, C. J.; Kim, B. J.; Bang, J. *Macromolecules* **2010**, *43*, 3570.
(55) Kim, B. J.; Fredrickson, G. H.; Kramer, E. J. *Macromolecules* **2008**, *41*, 436.
(56) Bai, L.; Ma, X.; Liu, J.; Sun, X.; Zhao, D.; Evans, D. G. *J. Am. Chem. Soc.* **2010**, *132*, 2333.

(57) Mezzenga, R.; Ruokolainen, J.; Fredrickson, G. H.; Kramer, E. J.; Moses, D.; Heeger, A. J.; Ikkala, O. *Science* **2003**, *299*, 1872.
(58) Niu, Z.; He, J.; Russell, T. P.; Wang, Q. *Angew. Chem., Int. Ed.* **2010**, *49*, 10052.
(59) Wu, S. *J. Polym. Sci., Part C: Polym. Symp.* **1971**, *34*, 19.
(60) Comyn, J. *Int. J. Adhes. Adhes.* **1992**, *12*, 145.
(61) Kang, D. J.; Kang, H.; Kim, K. H.; Kim, B. J. *ACS Nano* **2012**, *6*, 7902.